Histol Histopathol (2022) 37: 669-680

https://www.hh.um.es

Histology and Histopathology
From Cell Biology to Tissue Engineering

ORIGINAL ARTICLE **Open Access**

Tropomyosin 2 exerts anti-tumor effects in lung adenocarcinoma and is a novel prognostic biomarker

Peng Duan[1], Jing Cui[2], Hongyan Li[1] and Lei Yuan[3]

[1]Department of Oncology, [2]Department of Emergency and [3]Department of Respiratory, The Third People's Hospital of Qingdao, Qingdao, China

Summary. Background. Tropomyosin 2 (TPM2), a member of the actin filament binding protein family, plays distinct roles in the progression of different cancer types. Until now, there has been no study reporting TPM2 expression nor its function in lung adenocarcinoma (LUAD).

Methods. In the present study, we examined the expression profile of TPM2 by immunohistochemistry (IHC). The clinical significance of TPM2 was assessed by univariate and multivariate analyses. Function of TPM2 in LUAD was evaluated by knockdown and overexpression strategies in three LUAD cell lines, followed by proliferation and invasion assays. Xenografts were conducted in nude mice to further validate the tumor-related role of TPM2.

Results. Our results showed that TPM2 was downregulated in LUAD specimens and the low expression of TPM2 was associated with poor outcomes of LUAD patients. Overexpressing TPM2 inhibited cell proliferation and invasion of LUAD cell lines, while silencing TPM2 exerted the opposite effects. The effects of TPM2 in LUAD were further confirmed by xenograft assays.

Conclusions. Our results indicated that TPM2 exerted an anti-oncogenic role in LUAD via inhibiting tumor progression, thus providing a novel direction for the prognostic prediction and disease treatment.

Key words: Tropomyosin 2, Lung adenocarcinoma, Prognosis, Proliferation, Invasion

Introduction

Lung cancer ranks as the most common cancer and the leading cause of cancer-related death worldwide (Siegel et al., 2016). Among all cases, approximately 85% are classified as non-small cell lung cancer (NSCLC), mainly including lung adenocarcinoma (LUAD) and lung squamous carcinoma. Among them, LUAD accounts for more than 50% and is the most common and most aggressive histology type of lung cancer (Gridelli et al., 2015). Even though great improvements have been made in treatment therapies, the survival of patients with LUAD remains unsatisfactory (Diaz-Garcia et al., 2013). Therefore, identifying new biomarkers for prognosis prediction and therapeutic development is critically needed.

Tropomyosin 2 (TPM2) is a member of the actin filament binding protein family, playing roles in modulating the actin and myosin interaction. TPM2 is widely expressed in human tissues and its mutation or dysregulated expression can result in various diseases. For example, decreased expression of TPM2 may lead to heart failure and polycystic ovary syndrome (Li et al., 2016), while TPM2 mutation is closely correlated with congenital cap myopathy and nemaline myopathy (Tajsharghi et al., 2007). TPM2 can also collaborate with fibronectin to promote TGF-β1-induced contraction of human lung fibroblasts, thus may represent a novel therapeutic target in lung fibrosis (Bradbury et al., 2021). Interestingly, TPM2's downregulation was reported to suppress hepatitis virus B (HBV) production, which may affect liver carcinogenesis (Rahman et al., 2020). Indeed, the tumor-related role of TPM2 has been reported recently. Positive expression of TPM2 was reported to be associated with poorer overall survival of chronic lymphocytic leukemia (van't Veer et al., 2006). Bioinformatics analysis revealed a higher level of TPM2 in early-onset colorectal cancers than healthy controls (Zhao et al., 2019), and higher TPM2 indicated poorer overall survival of colon cancer patients (Gao et al., 2019; Liu et al., 2021b), highlighting its role in promoting cancer progression.

Contradictorily, TPM2 was reported to be downregulated in colorectal cancer tissues compared to normal colon tissues in other studies (Ma et al., 2016). TPM2-mRNA was also downregulated in prostate cancer and correlated with unfavorable prognosis (Varisli, 2013). Similarly, based on mass spectrometry data, TPM2 showed lower protein levels in bladder cancer

Corresponding Author: Lei Yuan, No. 29 Yongping Road, Licang District, Qingdao 266000, China. e-mail: yue730336939225928@163.com

DOI: 10.14670/HH-18-514

tissues and esophageal squamous cell carcinomas (ESCC) than adjacent nontumorous tissues (Zaravinos et al., 2011; Zhang et al., 2011). Consistently, RT-qPCR data also revealed decreased TPM2-mRNA levels in bladder cancer and ESCC (Chen et al., 2011; Zare et al., 2012), which may act as a tumor suppressor (Wu et al., 2021). In addition, Dube's data revealed a decreased expression of TPM2β-mRNA in breast cancer cell lines, which may be associated with decreased stress fiber formation and malignant transformation in human breast epithelial cells (Dube et al., 2016). On the other hand, the mRNA level of TPM2 showed no statistically significant difference between renal cell carcinoma and adjacent normal renal tissues (Wang et al., 2015). Therefore, the tumor-related role of TPM2 seems completely different in different malignancies. Until now, there have been no studies reporting the relationship between TPM2 and LUAD. Here we aimed to investigate its expression profile, clinical significance, and detailed functions in LUAD.

Materials and methods

Ethics

This study has been approved by the Ethic Committee of The Third People's Hospital of Qingdao. Each participant or direct relative fully understood and signed an informed consent form. The animal experimental protocol was approved by the Ethic Committee of The Third People's Hospital of Qingdao.

Online data mining

The mRNA level of *TPM2* was obtained from TCGA and GTEx datasets, which included 483 LUAD samples and 347 normal lung samples. The mRNA levels were presented as transcript per million (TPM) and compared by Student's t-test. Kaplan-Meier (KM) Plotter Server (http://kmplot.com) was used to determine the prognostic significance of *TPM2*.

Patient enrollment

In this study, we retrospectively enrolled 181 early stage LUAD patients that underwent curative surgical resection in our hospital. All cases were pathologically diagnosed as LUAD with TNM stage I-II. Patients who underwent preoperative neoadjuvant therapy or multiple tumor lesions were excluded. The age at the time of diagnoses was 66.0±11.0 years old, ranging 43-87 years old. Among all cases, 93 were female and 88 were male. Most cases showed tumor location in the right lung (113/181, 62.4%) and only 68 tumors showed left lung localization. Similarly, 124 cases showed upper lobe tumor location, while only 57 cases showed middle or lower lobe location. The mean tumor size was 2.6±1.8 cm in diameter, ranging from 0.5-9.0 cm. As for the tumor differentiation, 40 cases were classified as well differentiated, 91 cases as moderate differentiated, and the other 50 cases with poor differentiation. 105 cases were staged as T1, 63 cases as T2, and the other 13 cases with T3. Meanwhile, lymph node was positive in only 17 cases, while the other 164 cases showed negative lymph nodes. Accordingly, 97 cases were staged as TNM stage Ia, 49 cases as TNM stage Ib, and the other 35 cases with TNM stage II. We also collected the postoperative adjuvant chemotherapy information, which showed that 26 cases underwent adjuvant chemotherapy, while the other 155 patients rejected were not sure.

Immunohistochemistry (IHC)

The tumor tissues from all 181 cases were formalin-fixed paraffin-embedded (FFPE) and were used for IHC staining to evaluate TPM2 protein level in LUAD. Briefly, FFPE tissue sections were firstly de-paraffinized with xylene and ethanol. Secondly, sections were incubated in 3% H_2O_2 for 30 minutes to inactivate endogenous peroxidase and then incubated in EDTA buffer (pH=9.0) for antigen retrieval. Thirdly, unspecific antigen binding was blocked by 1% bovine serum albumin (BSA). Fourthly, polyclonal antibody TPM2 (1:300, 11038-1-AP, Thermo Fisher Scientific) was used to incubate slide sections. Finally, secondary antibody and DAB solution (Beyotime, Beijing, China) were used to visualize immunoreactivities (Liu et al., 2017).

The IHC results were next scored based on both staining intensity and the percentage of positively stained cells. Staining intensity score was given as negative staining: 1; weak staining: 2; moderate staining: 3; and strong staining: 4. Percentage of positive cells was scored as 0-25%: 1; 26-50%: 2; 51-75%: 3; and >75%: 4. The immunoreactivity score was obtained by multiplying the two scores above, ranging from 1-16. To better evaluate the clinical significance of TPM2, we classified patients into low-TPM2 expression group (score <6, n=92) and high-TPM2 expression group (score ≥6, n=89) based on the median immunoreactivity score.

Cell culture and transfection

Human LUAD cell lines (PC9 and H1975) were obtained from the American Type Culture Collection (ATCC). All cells were maintained in RPMI-1640 medium supplemented with 10% fetal bovine serum (FBS) and penicillin-streptomycin, and cultured in an incubator with a humidified atmosphere of 5% CO_2 at 37°C.

TPM2-specific shRNA in pLKO.1-puro vector was used for knockdown assays, while TPM2-pcDNA3.0 plasmids were used for overexpression assays. Both the shRNA and plasmids were synthesized by Genechem (Shanghai, China). The transfection of shRNA and plasmids were conducted as described by others using untreated cells as blank control (Liu et al., 2021a).

PCDNA3.0-vector and pLKO.1-puro vector were used for the control in overexpression and knockdown assays, respectively.

Western blot

WB was used to test protein expression levels. Briefly, NP40 lysis buffer was used to lyse cells and extract proteins, followed by protein quantification and denaturing. Then the same amount of protein samples was separated by SDS-PAGE (sodium dodecyl sulphate-polyacrylamide gel electrophoresis) and transferred onto the PVDF (polyvinylidene fluoride) membrane, followed by incubation with primary antibody (1:1000 dilution) and secondary antibody (1:10,000 dilution). The protein expression level was finally visualized by testing the immunoreactivity of the PVDF membrane using enhanced chemiluminescence (ECL) reagent (Chen et al., 2021b).

3-(4,5-dimethylthiazol-2-yl)-2,5-diphenyl tetrazolium bromide (MTT) assay

Cells were reseeded on 96-well plates at 3000 cells/well and cell proliferation was determined by MTT assay at daily intervals for five days. At each time point, 20 μL of 5 mg/ml MTT was added to each well and incubated for another 4 hours, then the culturing medium was discarded and 150 μL DMSO was added to dissolve the precipitated formazan. Absorbance was measured at 490 nm. Each experiment was repeated three times.

Colony formation

Single-cell suspensions of LUAD cells were seeded into 6-well plates at 400 cells/well and incubated at 37°C for 14 days. Then cells were fixed with 4% formaldehyde for 30 min and stained by 0.1% crystal violet solution for another 30 min. The number of stained colonies in each well was counted. Each experiment was repeated three times.

Transwell migration and invasion assays

Cells were resuspended in RPMI 1640 medium (500 μL) containing 5% FBS and placed in the upper chamber inserts of transwell plates (Corning, Merck Life Science) at 1×10^5 cells/well for migration assay. The same amount of medium containing 20% FBS was added to the lower chamber inserts and then cultured for 24 h at 37°C. Then the medium was discarded, and cells attached to the lower side of membrane were stained with crystal violet and counted using a light microscope (Cao et al., 2020). For the invasion assay, the same strategy was used except that the inserts were precoated with 20 μg Matrigel (BD Biosciences) and the culturing time was 48h (Deng et al., 2020). Each experiment was repeated three times and normalized according to the total proliferated cell number.

Xenografts

The animal experimental protocol was conducted following the laboratory animal welfare. Briefly, BALB/c nu/nu mice (4 weeks old) were purchased from the Shanghai Institute of Materia Medical, and housed under specific pathogen-free conditions as required. Mice were randomly assigned to = knockdown group, or overexpression group, or control groups. A total of 10^7 stably transfected cells in 0.2 mL PBS were implanted by subcutaneous injection to obtain the corresponding subcutaneous tumors. The tumor growth was monitored by calculating tumor volume. The growth of xenografts was monitored by using a Vernier caliper. All mice were sacrificed to obtain xenografts once the largest diameter was larger than 10 mm.

Statistics

Cancer-specific survival (CSS) was defined as the period from the date of surgical resection to the date of death from LUAD or the date of last follow-up, ranging from 1-85 months. Statistical analyses were performed using the SPSS Software. The association between TPM2 protein level and clinical characteristics were evaluated through Chi-square test. Kaplan–Meier analysis and log-rank test were used to analyze and plot the survival curves of enrolled LUAD patients. Independent prognostic factors were identified by using the multivariate Cox regression model. Student's t-test was used to compare cellular data. $P<0.05$ was considered statistically significant. * indicates $P<0.05$, ** indicates $P<0.01$, *** indicates $P<0.001$.

Results

TPM2-mRNA level in LUAD and its prognostic significance

The mRNA level of TPM2 in LUAD tissues and normal lung tissues were retrieved from TCGA and GTEx datasets, which revealed that *TPM2-mRNA* was significantly downregulated in LUAD tissues ($P<0.001$, Fig. 1A). Moreover, Kaplan-Meier survival analysis showed that patients with lower *TPM2* exhibited poorer survival time ($P=0.004$, Fig. 1B). Therefore, online data mining suggested a potential anti-tumor role of *TPM2* in LUAD.

TPM2 protein expression and its correlation with clinicopathological characteristics

We next conducted IHC experiments to explore the protein expression profile of TPM2 in LUAD, which identified distinct expression levels in different tumor tissues (Fig. 1C). Therefore, we sub-grouped our cohort into low-TPM2 protein expression group (n=92), and high-TPM2 group (n=89). The clinical relevance of TPM2 was firstly evaluated by Chi-square tests.

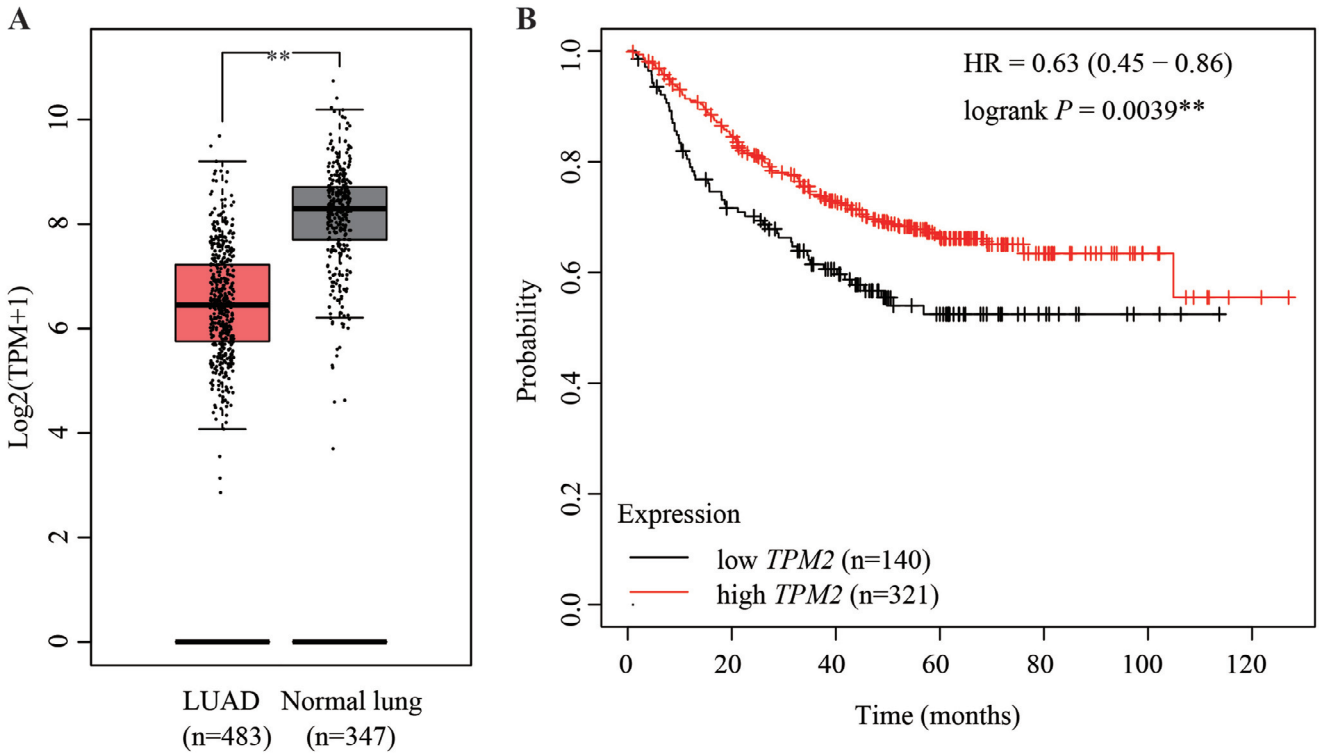

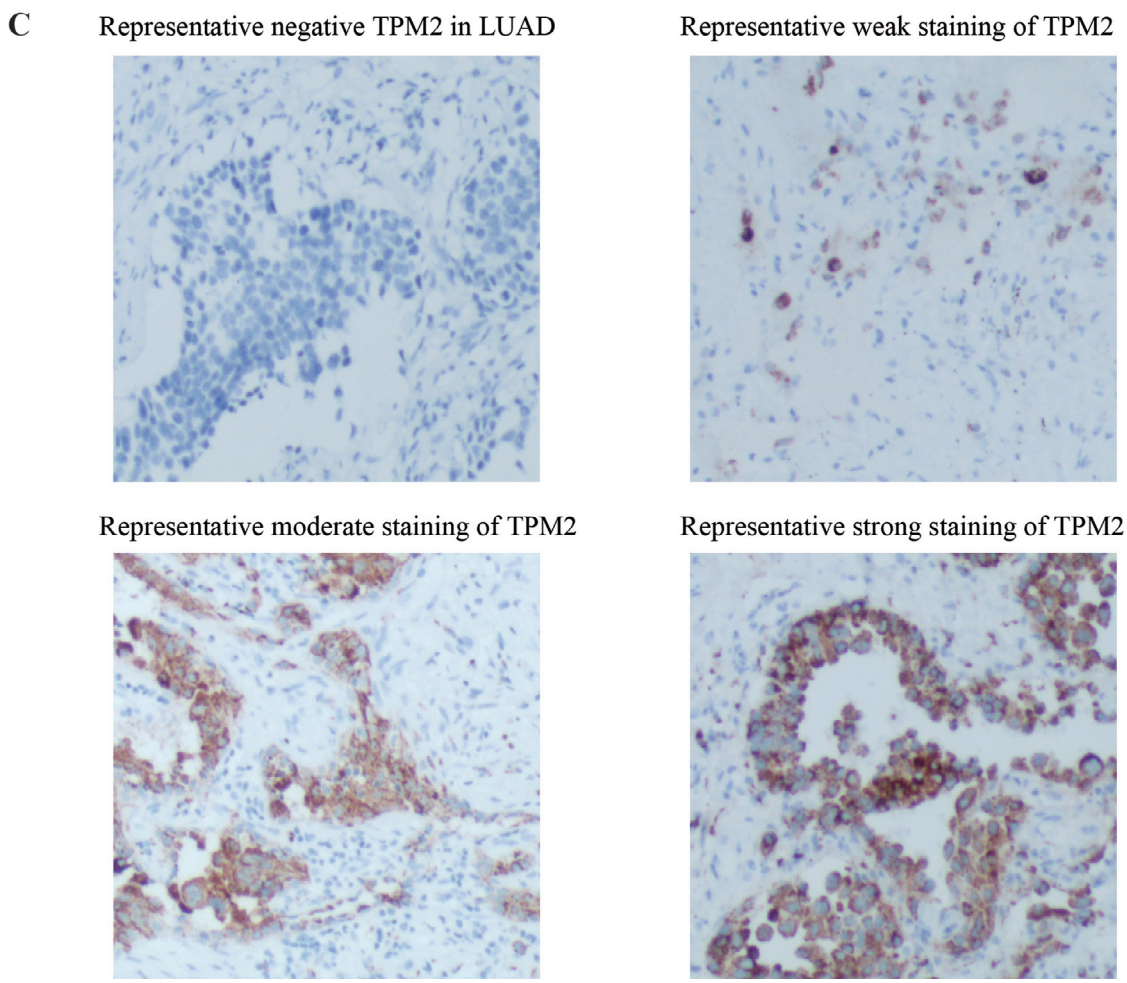

Fig. 1. Expression of *TPM2* in LUAD. **A.** mRNA levels of TPM2 in LUAD tissues (n=483) and normal lung tissues (n=347) were obtained from TCGA and GTEx datasets, which revealed a lower *TPM2* level in LUAD tissues as presented by transcript per million (TPM). * indicates P<0.05 by Student's t-test. **B.** Kaplan-Meier survival analysis was conducted to test the prognostic role of TPM2-mRNA in LUAD. Accordingly, patients with lower *TPM2* level exhibited poorer survival (P=0.004). * indicates P<0.05 by log-rank test. **C.** Representative IHC images of negative, weak, moderate, and strong TPM2 staining in LUAD tissues. x 400.

Accordingly, TPM2 showed a negative correlation with tumor size (P<0.001, Table 1). The tumor size of high-TPM2 group was 1.9±1.0 cm, while this increased to 3.3±2.2 cm in the low-TPM2 group. Meanwhile, tissues with poorer differentiation grade exhibited lower TPM2 level (P=0.038). Patients with lower TPM2 expression levels were also prevalent to exhibit more advanced T stages (P<0.001). Of note, up to 76.5% (13/17) LN-positive cases showed low TPM2 expression, while only 48.2% (79/164) LN-negative ones were classified as low-TPM2 patients (P=0.026). Consistent with T stage and LN metastasis, the TNM stage also showed negative correlation with TPM2 expression (P<0.001). The relevance between TPM2 expression with patients' characteristics indicated that lower TPM2 may be correlated with LUAD progression.

Table 1. Characteristics of the LUAD patients and their associations with TPM2 protein expression.

Variable	Cases	TPM2 expression		P value
	(n=181)	High (n=89)	Low (=92)	
Age (years)				
Mean±SD	66.0±11.0	65.5±12.1	66.4±9.9	0.338
≤ 60 yrs	87	46	41	
> 60 yrs	94	43	51	
Sex				
Male	88	48	40	0.159
Female	93	41	52	
Side				
Left	68	36	32	0.431
Right	113	53	60	
Location				
Upper lobe	124	65	59	0.197
Middle/lower lobe	57	24	33	
Size (cm)				
Mean±SD	2.6±1.8	1.9±1.0	3.3±2.2	
<0.001***				
≤ 2.0 cm	86	69	17	
> 2.0 cm	95	20	75	
Differentiation				
Well	40	26	14	0.038
Moderate	91	44	47	
Poor	50	19	31	
T stage				
T1	105	63	42	<0.001
T2	63	25	38	
T3	13	1	12	
LN metastasis				
Negative	164	85	79	0.026
Positive	17	4	13	
TNM stage				
Ia	97	61	36	<0.001
Ib	49	22	27	
II	35	6	29	
Adjuvant chemotherapy				
No or unknown	155	82	73	0.014
Yes	26	7	19	

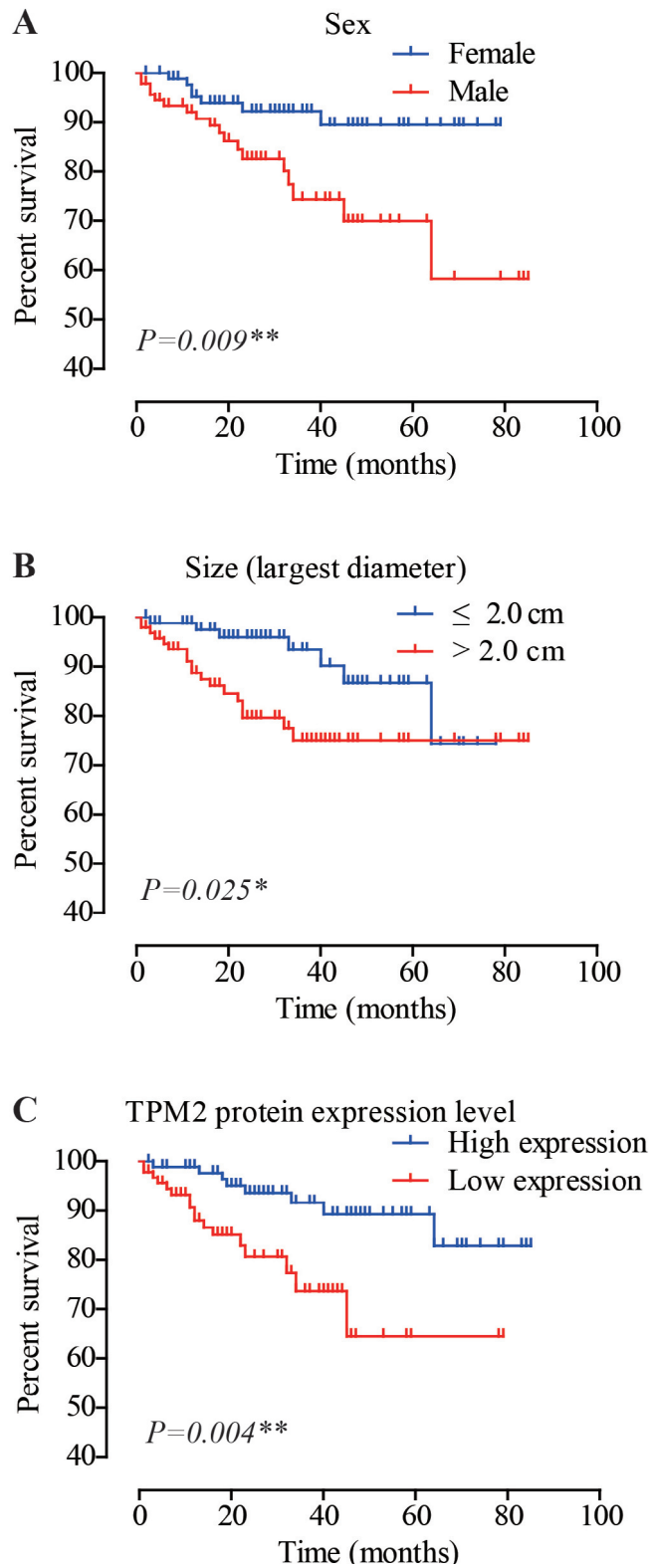

Fig. 2. Cancer-specific survival (CSS) analyses of LUAD cohort. The CSS curves were plotted according to patients' sex **(A)**, tumor size **(B),** and TPM2 protein level **(C)**. * indicates P<0.05 by log-rank test.

TPM2 is a novel biomarker for prognostic prediction of LUAD

Univariate analysis was then performed to assess the prognostic role of each parameter (Table 2). Accordingly, female patients showed shorter CSS time (63.9±4.4 months) than male patients (72.9±2.2 months, Fig. 2A, P=0.009). Larger tumor size was also an unfavorable prognostic factor (Fig. 2B, P=0.025). Moreover, the mean CSS time for low-TPM2 group was only 59.7±4.5 months, while it was 77.1±2.6 months for high-TPM2 group (Fig. 2C, P=0.037).

To better validate our clinical findings, we also selected the Cox regression model to conduct multivariate analysis for all variables (Table 2). As a result, female patients (P=0.046) and middle/lower lobe tumor location (P=0.035) both help predict poorer prognosis. Moreover, lower TPM2 expression level was also identified as an independent prognostic factor for poorer CSS of LUAD patients (P=0.037, Table 2).

TPM2 exerts anti-tumor effects in LUAD cells

Two LUAD cell lines (PC9 and H1975) were used for overexpression of TPM2 (Fig. 3A). After validating the transfection efficiencies, both cell lines were subjected to MTT assays to evaluate cell proliferation. As a result, TPM2-overexpression inhibited cell growth (Fig. 3B). Consistently, colony formation assays revealed that the colony formation capacity of TPM2-overexpression group was significantly impaired compared with control group (Fig. 3C). Considering the clinical relevance between TPM2 expression with lymph node metastasis, we next conducted migration and

Table 2. Univariate and multivariate analyses for the cancer specific survival (CSS) of LUAD patients.

Variable	Cases	Overall survival		Univariate	Multivariate
	(n = 116)	Mean±SD (Months)	5-year (%)	P value	P value
Age (years)				0.786	
≤ 60 yrs	87	70.1±3.5	80.4%		
> 60 yrs	94	72.8±3.3	80.4%		
Sex				0.009	0.023
Male	88	72.9±2.2	89.5%		
Female	93	63.9±4.4	70.0%		
Side				0.802	
Left	68	70.4±3.7	78.1%		
Right	113	71.6±3.5	82.4%		
Location				0.180	
Upper lobe	124	73.4±2.8	83.3%		
Middle/lower lobe	57	62.9±4.3	73.7%		
Size (cm)				0.025*	0.454
≤ 2.0 cm	86	70.1±2.8	86.7%		
> 2.0 cm	95	67.9±3.6	75.0%		
Differentiation				0.439	
Well	40	69.5±4.0	86.2%		
Moderate	91	66.8±3.2	79.9%		
Poor	50	67.4±5.2	72.9%		
T stage				0.113	
T1	105	73.5±2.9	88.0%		
T2	63	64.7±4.9	67.2%		
T3	13	63.6±10.7	69.9%		
LN metastasis				0.682	
Negative	164	71.7±2.7	80.7%		
Positive	17	70.1±7.3	79.1%		
TNM stage				0.181	
Ia	97	72.9±3.1	87.0%		
Ib	49	61.5±4.3	73.0%		
II	35	64.2±6.3	68.4%		
Adjuvant chemotherapy				0.057	
No or unknown	155	73.8±2.5	81.8%		
Yes	26	61.3±7.0	71.7%		
TPM2 expression				0.004	0.046
High	89	77.1±2.6	89.3%		
Low	92	59.7±4.5	64.5%		

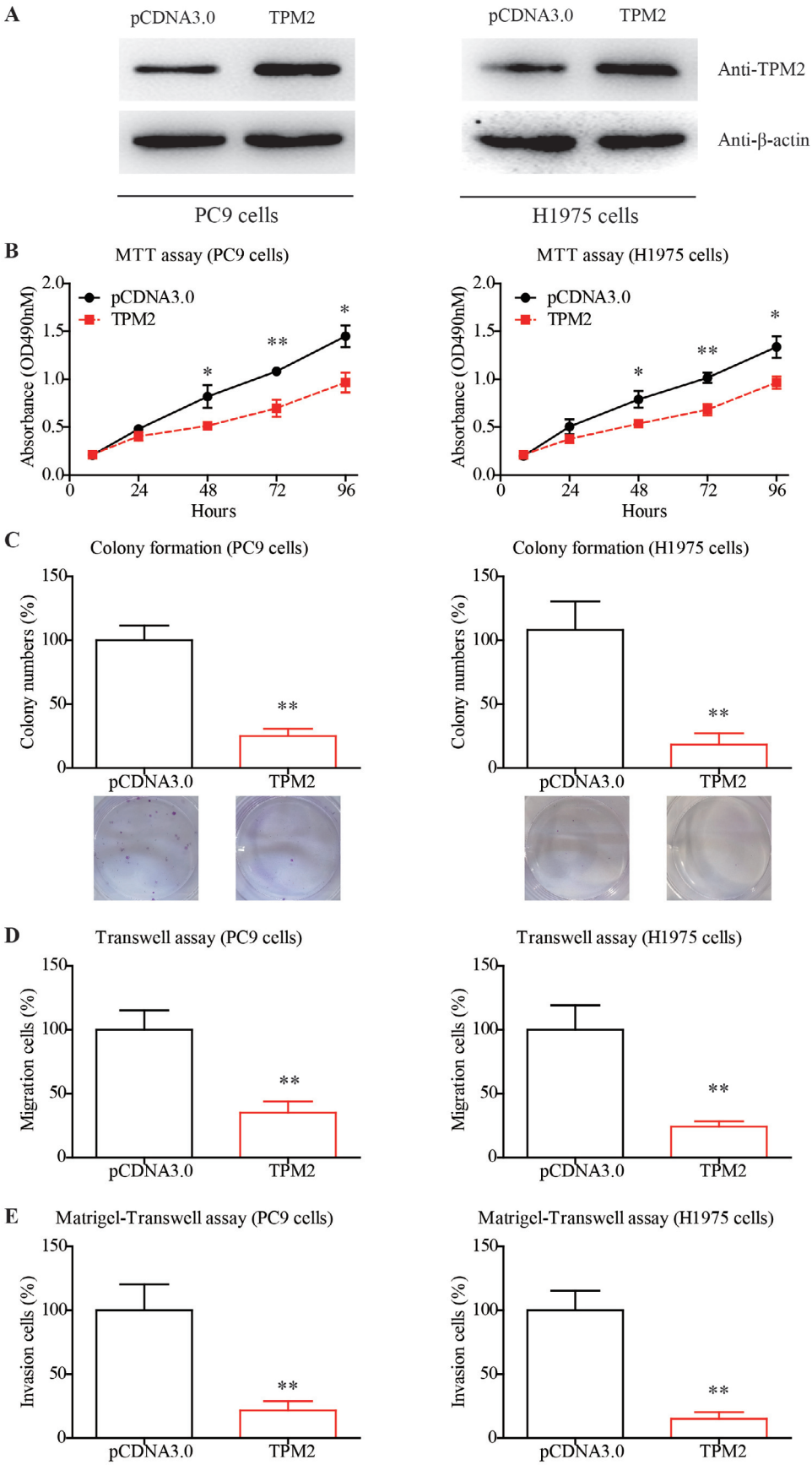

Fig. 3. Overexpressing TPM2 exerts anti-tumor effects in LUAD cells. **A.** Transfection efficiencies of TPM2-overexpression and vector control cells were tested via Western blotting in PC9 and H1975 cells, respectively. **B.** MTT experiments were conducted to test the effects of TPM2-overexpression on LUAD cell proliferation. **C.** Colony formation assays were used to validate the growth capacities of transfected LUAD cells. **D.** Migration capacities of LUAD cell lines were tested by Transwell assays. **E.** Invasion capacities of LUAD cell lines were evaluated by Matrigel-Transwell assays. Data are presented as Mean±SD from three independent repeats. * indicates P<0.05 by Student's t-test compared with control groups.

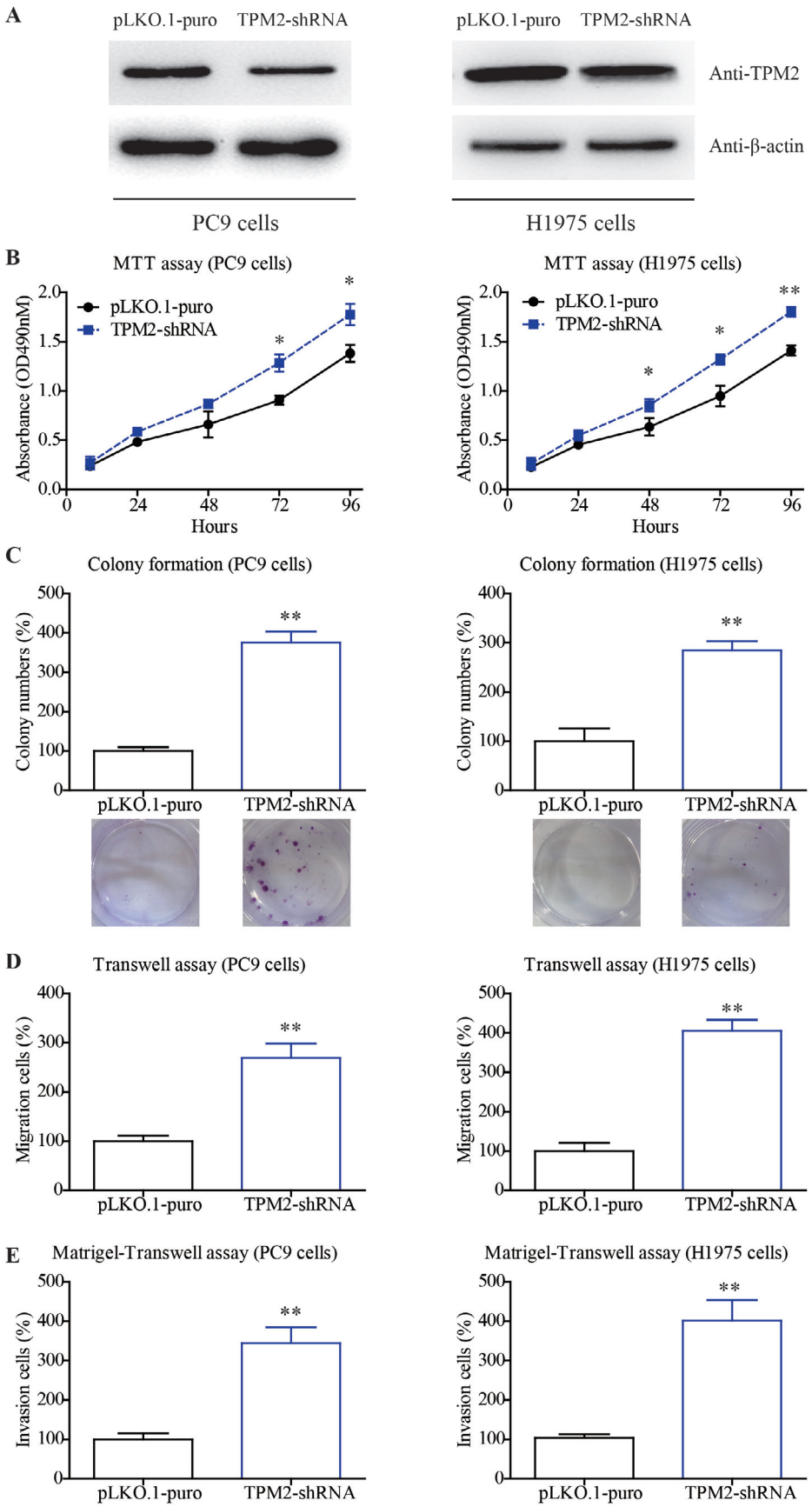

Fig. 4. Silencing TPM2 enhances growth and invasion of LUAD cells. **A.** Transfection efficiencies of TPM2-knockdown and vector control cells were tested via Western blotting in PC9 and H1975 cells, respectively. **B.** MTT experiments were conducted to test the effects of TPM2-knockdown on LUAD cell proliferation. **C.** Colony formation assays were used to validate the growth capacities of transfected LUAD cells. **D.** Migration capacities of LUAD cell lines were tested by Transwell assays. **E.** Invasion capacities of LUAD cell lines were evaluated by Matrigel-Transwell assays.Data are presented as Mean±SD from three independent repeats. *indicates $P<0.05$ by Student's t-test compared with control groups.

invasion tests. As expected, TPM2-overexpression impaired the migration and invasion capacities of LUAD cells (Fig. 3D,E).

In addition to overexpression assays, we also conducted knockdown experiments using specific shRNA targeting TPM2 (Fig. 4A). In contrast with the effects induced by TPM2-overexpression, TPM2-shRNA resulted in accelerated cell growth (Fig. 4B), better colony formation (Fig. 4C), enhanced migration and invasion capacities (Fig. 4D,E).

TPM2 inhibits LUAD growth in vivo

To further validate the tumor-related role of TPM2, we finally performed xenograft experiments using a mouse model. We subcutaneously injected control PC9 cells transfected with vectors, TPM2-overexpressed PC9 cells, and TPM2-knockdown PC9 cells into the nude mice, respectively. Similarly, H1975 cells were used to generate a xenograft model. According to the growth curve of xenografts, overexpressing TPM2 significantly inhibited LUAD tumor growth, while knockdown of TPM2 promoted tumor growth in vivo (Fig. 5A). Consistent with growth curves, the isolated xenografts also showed macroscopical differences among different groups (Fig. 5B). Finally, the isolated xenografts were weighed and revealed that TPM2-overexpression led to impaired tumor growth (Fig. 5C), thus emphasizing the tumor-suppressing role of TPM2 in LUAD.

Discussion

The tumor-related role of TPM2 remains controversial in different tumor types. On one hand, TPM2 exerts oncogenic effects and promotes cancer progression. According to proteomic analysis, the protein level of TPM2 was upregulated in a highly metastatic variant of human MDA-MB-435 breast cancer cell line compared with parental MDA-MB-435 cells, indicating its potential role in promoting metastatic progression (Li et al., 2006). Interestingly, single-cell multiomics also showed that compared with fibroblasts from adjacent normal tissues, fibroblasts from primary colon cancers exhibited higher TPM2 expression, whose higher level was correlated with poorer overall survival (Zhou et al., 2020). The alteration of TPM2 in tumor stromal cells provided evidence of TPM2's effects in tumor microenvironments. Besides, acetylome revealed a distinct level of TPM2 acetylation in colorectal cancer and its liver metastasis, highlighting the importance of TPM2 post-translational modification (Shen et al., 2016; Tang et al., 2018; Wang and Wang, 2021). Moreover,

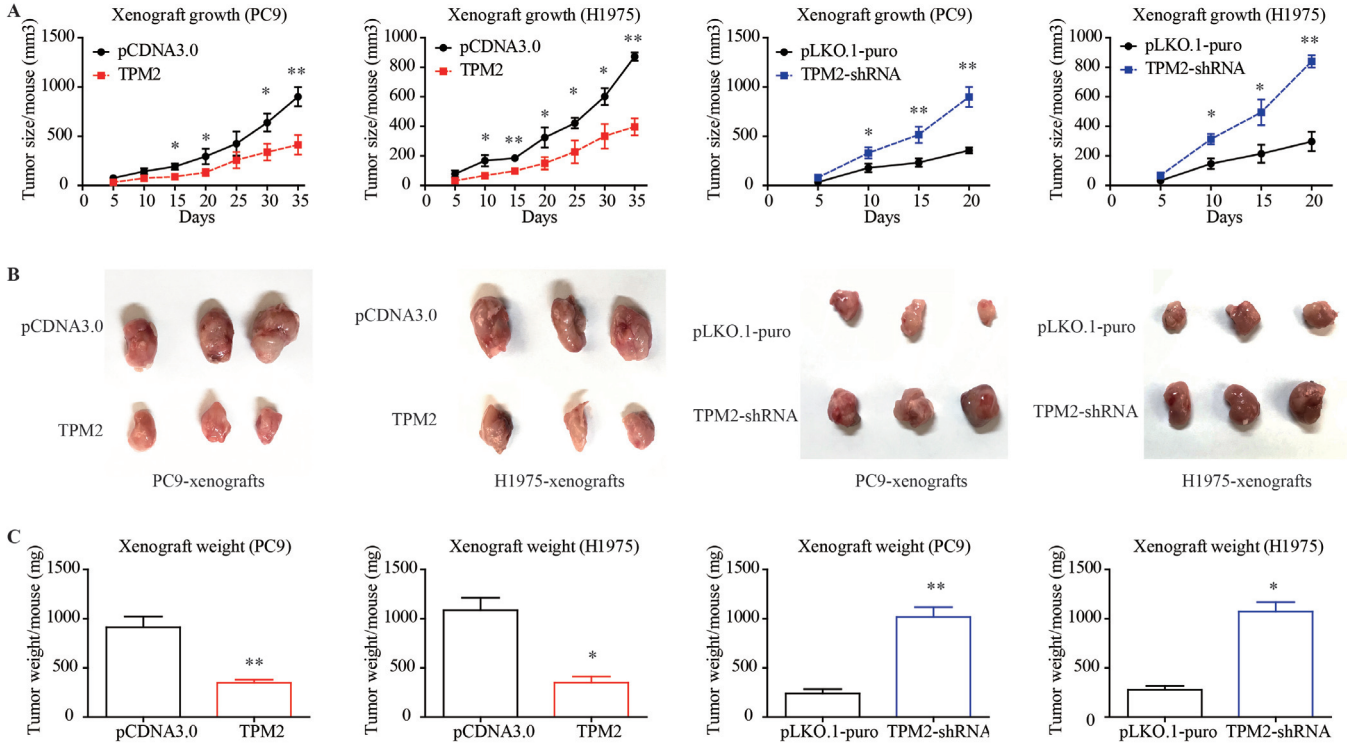

Fig. 5. TPM2 inhibits LUAD growth in vivo. Transfected PC9 or H1975 cells were subcutaneously injected into nude mice, then the xenograft volumes were monitored every five days **(A)**. Once the largest diameter was larger than 10mm in the group, all mice were sacrificed to isolate the xenografts for picturing **(B)** and weighting **(C)**. Data are presented as Mean±SD from three independent repeats. * indicates P<0.05 by Student's t-test compared with control groups.

siRNA targeting TPM2 was identified as an effective inducer of non-apoptotic cell death by modulating lysosomal membrane permeabilization and lysosomal localization, indicating TPM2's function on protecting cell survival. Importantly, TPM2-siRNA killed human cervix cancer and osteosarcoma cells and sensitized them to lysosome-destabilizing treatments, such as photo-oxidation, siramesine, etoposide or cisplatin. Clinically, although the upregulated level of TPM2 itself showed no significance on predicting survival of oral squamous cell carcinoma (OSCC), its combination with another three upregulated genes can help predict unfavorable outcomes of OSCC (Vincent-Chong et al., 2017). Similarly, Zhao and his colleagues also selected higher TPM2 as an important component in their risk model to predict poorer overall survival of OSCC (Zhao et al., 2021). Therefore, TPM2 can function as a tumor promoter and targeting TPM2 may serve as a novel therapeutic direction for certain malignancies.

However, TPM2 seems to play anti-tumor roles in other malignancies. For example, treating with conditioned medium from BM-MSCs inhibited the proliferation of C6 glioma cells but promoted their migration and invasion. Interestingly, TPM2 was downregulated in the treated cells. Considering that TPM2 was associated with motility and the cytoskeleton, the altered phenotypes of treated C6 glioma cells may be closely correlated with TPM2 (Li et al., 2021). However, the detailed function needs to be further clarified. Indeed, a previous study reported a decreased expression level of TPM2 in the invasive stages of small-intestinal neuroendocrine tumors (SI-NETs) compared with the pre-invasive stages (Couderc et al., 2015), indicating that TPM2 may attenuate tumor metastasis. Consistently, our clinical data also showed that TPM2 was negatively correlated with tumor size and lymph node metastasis in our enrolled LUAD cohort. Furthermore, cellular and mice studies demonstrated its role on attenuating LUAD proliferation and metastasis both in vitro and in vivo.

Although we did not dig into the detailed functional mechanism, the involved signaling pathways may be partially reflected by other studies and deserve further investigation by multiple-omics methods (Chen et al., 2021a; Zou et al., 2021). For example, TPM2 can suppress cell proliferation in colorectal cancer cell lines, whereas the loss of TPM2 expression is associated with increased tumor proliferation, which was accompanied by RhoA activation (Cui et al., 2016). Beyond cell proliferation, TPM2 can also regulate sensitivity to apoptosis by modulating the expression of key intrinsic apoptosis proteins which primes cell death of rat neuroepithelial cells (Desouza-Armstrong et al., 2017). Meanwhile, loss of TPM2 also facilitates the metastatic potential of MCF10A breast cells by enhancing actomyosin contractility and increasing the expression of E-cadherin and β-catenin (Shin et al., 2017). Similarly, absence of TPM2 was reported to facilitate elongated mesenchymal invasion of primary patient-derived glioblastomas by modulating actin cytoskeleton organization (Mitchell et al., 2019). Consistent with TPM2's oncogenic role, its upstream microRNA miR-183-5p. can promote the migration and invasion of glioblastoma cells as well as inhibit cell apoptosis by targeting TPM2 (Lin et al., 2019).

Clinically, we provided the initial evidence on that TPM2 was downregulated in LUAD tissues compared with normal lung tissues and its lower expression was correlated with unfavorable prognosis. Interestingly, the hypoxia-induced methylation of TPM2 has been reported to downregulate TPM2 expression and lead to poor prognosis of breast cancer (Zhang et al., 2018). Similarly, aberrant high TPM2 methylation was observed in colon cancer, which resulted in decreased TPM2 expression and poorer survival (Cui et al., 2016). Considering that TPM2 can also enhance chemo-resistance to paclitaxel in breast cancer (Zhang et al., 2018), future studies focusing on the methylation status of TPM2 in LUAD may provide novel directions for therapeutic development.

Besides prognostic prediction, TPM2 may also serve as a diagnostic biomarker. For example, TPM2 is significantly elevated in ovarian cancer patient sera compared with controls according to proteomic results (Tang et al., 2013). Similarly, higher serum TPM2 level was also reported to possess diagnostic potential for endometriosis (Irungu et al., 2019). Therefore, testing the serum level of TPM2 in pan-cancers may also help widen our knowledge regarding TPM2's clinical significance. Another limitation of our study is that here we only enrolled early-stage LUAD cases. It will be helpful to validate our findings by testing its clinical significance in late-stage LUADs and provide evidence regarding its correlation with adjuvant therapy resistance.

Conclusions

TPM2 exerted an anti-oncogenic role in LUAD via inhibiting tumor progression, thus providing a novel direction for the prognostic prediction and treatment of LUAD.

Author contributions. Peng Duan conducted clinical data analyses; Jing Cui conducted cellular experiments; Hongyan Li performed xenograft experiments; Lei Yuan designed this project.
Funding. None.
Conflict of Interest. None.
Data availability. Data will be available upon request.

References

Bradbury P., Nader C.P., Cidem A., Rutting S., Sylvester D., He P., Rezcallah M.C., O'Neill G.M. and Ammit A.J. (2021). Tropomyosin 2.1 collaborates with fibronectin to promote TGF-β 1-induced contraction of human lung fibroblasts. Respir. Res, 22, 1-10.

Cao H., Zheng J., Yao Y., Yang Q., Yan R., Sun W., Ruan K., Zhou J. and Zhou J. (2020). Overexpression of KIAA0101 promotes the

progression of non-small cell lung cancer. J. Cancer 11, 6663-6674.

Chen R., Feng C. and Xu Y. (2011). Cyclin-dependent kinase-associated protein Cks2 is associated with bladder cancer progression. J. Int. Med. Res. 39, 533-540.

Chen L., He M., Zhang M., Sun Q., Zeng S., Zhao H., Yang H., Liu M., Ren S. and Meng X. (2021a). The role of non-coding RNAs in colorectal cancer, with a focus on its autophagy. Pharmacol. Ther. 226, 107868.

Chen T., Liu H., Liu Z., Li K., Qin R., Wang Y., Liu J., Li Z., Gao Q. and Pan C. (2021b). FGF19 and FGFR4 promotes the progression of gallbladder carcinoma in an autocrine pathway dependent on GPBAR1-cAMP-EGR1 axis. Oncogene 40, 4941-4953.

Couderc C., Bollard J., Couté Y., Massoma P., Poncet G., Lepinasse F., Hervieu V., Gadot N., Sanchez J.-C. and Scoazec J.-Y. (2015). Mechanisms of local invasion in enteroendocrine tumors: Identification of novel candidate cytoskeleton-associated proteins in an experimental mouse model by a proteomic approach and validation in human tumors. Mol. Cell Endocrinol. 399, 154-163.

Cui J., Cai Y., Hu Y., Huang Z., Luo Y., Kaz A.M., Yang Z., Chen D., Fan X. and Grady W.M. (2016). Epigenetic silencing of TPM2 contributes to colorectal cancer progression upon RhoA activation. Tumour Biol. 37, 12477-12483.

Deng X., Xiong W., Jiang X., Zhang S., Li Z., Zhou Y., Xiang B., Zhou M., Li X. and Li G. (2020). LncRNA LINC00472 regulates cell stiffness and inhibits the migration and invasion of lung adenocarcinoma by binding to YBX1. Cell Death Dis. 11, 1-13.

Desouza-Armstrong M., Gunning P.W. and Stehn J.R. (2017). Tumor suppressor tropomyosin Tpm2. 1 regulates sensitivity to apoptosis beyond anoikis characterized by changes in the levels of intrinsic apoptosis proteins. Cytoskeleton 74, 233-248.

Diaz-Garcia C.V., Agudo-Lopez A., Perez C., Lopez-Martin J.A., Rodriguez-Peralto J.L., de Castro J., Cortijo A., Martinez-Villanueva M., Iglesias L., Garcia-Carbonero R., Fresno Vara J.A., Gamez-Pozo A., Palacios J., Cortes-Funes H., Paz-Ares L., Agulló-Ortuño M.T. (2013). DICER1, DROSHA and miRNAs in patients with non-small cell lung cancer: implications for outcomes and histologic classification. Carcinogenesis 34, 1031-1038.

Dube S., Thomas A., Abbott L., Benz P., Mitschow C., Dube D.K. and Poiesz B.J. (2016). Expression of tropomyosin 2 gene isoforms in human breast cancer cell lines. Oncol. Rep. 35, 3143-3150.

Gao Z., Fu P., Yu Z., Zhen F. and Gu Y. (2019). Comprehensive analysis of lncRNA–miRNA–mRNA network ascertains prognostic factors in patients with colon cancer. Technol Cancer Res. Treat, 18, 1533033819853237.

Gridelli C., Rossi A., Carbone D.P., Guarize J., Karachaliou N., Mok T., Petrella F., Spaggiari L. and Rosell R. (2015). Non-small-cell lung cancer. Nat. Rev. Dis. Primers 1, 15009.

Irungu S., Mavrelos D., Worthington J., Blyuss O., Saridogan E. and Timms J.F. (2019). Discovery of non-invasive biomarkers for the diagnosis of endometriosis. Clin. Proteomics 16, 1-16.

Li D.Q., Wang L., Fei F., Hou Y.F., Luo J.M., Zeng R., Wu J., Lu J.S., Di G.H. and Ou Z.L. (2006). Identification of breast cancer metastasis-associated proteins in an isogenic tumor metastasis model using two-dimensional gel electrophoresis and liquid chromatography-ion trap-mass spectrometry. Proteomics 6, 3352-3368.

Li L., Mo H., Zhang J., Zhou Y., Peng X. and Luo X. (2016). The role of heat shock protein 90B1 in patients with polycystic ovary syndrome. PLoS One 11, e0152837.

Li S., Xiang W., Tian J., Wang H., Hu S., Wang K., Chen L., Huang C. and Zhou J. (2021). Bone marrow-derived mesenchymal stem cells differentially affect glioblastoma cell proliferation, migration, and invasion: A 2D-DIGE proteomic analysis. Biomed. Res. Int. 2021, 4952876.

Lin J., Shen J., Yue H. and Cao Z. (2019). miRNA-183-5p. 1 promotes the migration and invasion of gastric cancer AGS cells by targeting TPM1. Oncol. Rep. 42, 2371-2381.

Liu H., Xu Y., Zhang Q., Yang H., Shi W., Liu Z., Li K., Gong Z., Ning S. and Li S. (2017). Prognostic significance of TBL1XR1 in predicting liver metastasis for early stage colorectal cancer. Surg. Oncol. 26, 13-20.

Liu H., Gong Z., Li K., Zhang Q., Xu Z. and Xu Y. (2021a). SRPK1/2 and PP1α exert opposite functions by modulating SRSF1-guided MKNK2 alternative splicing in colon adenocarcinoma. J. Exp. Clin. Cancer Res. 40, 1-16.

Liu S., Zeng F., Fan G. and Dong Q. (2021b). Identification of hub genes and construction of a transcriptional regulatory network associated with tumor recurrence in colorectal cancer by eeighted gene co-expression network analysis. Front Genet. 12, 495.

Ma Y., Xiao T., Xu Q., Shao X. and Wang H. (2016). iTRAQ-based quantitative analysis of cancer-derived secretory proteome reveals TPM2 as a potential diagnostic biomarker of colorectal cancer. Front. Med. (Lausanne) 10, 278-285.

Mitchell C.B., Black B., Sun F., Chrzanowski W., Cooper-White J., Maisonneuve B., Stringer B., Day B., Biro M. and O'Neill G.M. (2019). Tropomyosin Tpm 2.1 loss induces glioblastoma spreading in soft brain-like environments. J. Neurooncol. 141, 303-313.

Rahman M.A., Ueda K. and Honda T. (2020). A traditional Chinese medicine, maoto, suppresses hepatitis B virus production. Front. Cell. Infect. Microbiol. 10, 894.

Shen Z., Wang B., Luo J., Jiang K., Zhang H., Mustonen H., Puolakkainen P., Zhu J., Ye Y. and Wang S. (2016). Global-scale profiling of differential expressed lysine acetylated proteins in colorectal cancer tumors and paired liver metastases. J. Proteomics 142, 24-32.

Shin H., Kim D. and Helfman D.M. (2017). Tropomyosin isoform Tpm2. 1 regulates collective and amoeboid cell migration and cell aggregation in breast epithelial cells. Oncotarget 8, 95192.

Siegel R.L., Miller K.D. and Jemal A. (2016). Cancer statistics, 2016. CA Cancer J. Clin. 66, 7-30.

Tajsharghi H., Ohlsson M., Lindberg C. and Oldfors A. (2007). Congenital myopathy with nemaline rods and cap structures caused by a mutation in the β-tropomyosin gene (TPM2). Arch. Neurol. 64, 1334-1338.

Tang H.-Y., Beer L.A., Tanyi J.L., Zhang R., Liu, Q. and Speicher D.W. (2013). Protein isoform-specific validation defines multiple chloride intracellular channel and tropomyosin isoforms as serological biomarkers of ovarian cancer. J. Proteomics 89, 165-178.

Tang W., Wan S., Yang Z., Teschendorff A.E. and Zou Q. (2018). Tumor origin detection with tissue-specific miRNA and DNA methylation markers. Bioinformatics 34, 398-406.

van't Veer M.B., Brooijmans A.M., Langerak A.W., Verhaaf B., Goudswaard C.S., Graveland W.J., van Lom K. and Valk P. (2006) The predictive value of lipoprotein lipase for survival in chronic lymphocytic leukemia. Haematologica 91, 56-63.

Varisli L. (2013) Identification of new genes downregulated in prostate cancer and investigation of their effects on prognosis. Genet. Test

Mol. Biomarkers 17, 562-566.

Vincent-Chong V.K., Salahshourifar I., Woo K.M., Anwar A., Razali R., Gudimella R., Rahman, Z.A.A., Ismail S.M., Kallarakkal T.G. and Ramanathan A. (2017). Genome wide profiling in oral squamous cell carcinoma identifies a four genetic marker signature of prognostic significance. PLoS One 12, e0174865.

Wang Y. and Wang F. (2021). Post-translational modifications of deubiquitinating enzymes: expanding the ubiquitin code. Front. Pharmacol. 12, 1434.

Wang J., Guan J., Lu Z., Jin J., Cai Y., Wang C. and Wang F. (2015). Clinical and tumor significance of tropomyosin-1 expression levels in renal cell carcinoma. Oncol. Rep. 33, 1326-1334.

Wu H., Jiang W., Ji G., Xu R., Zhou G. and Yu H. (2021). Exploring microRNA target genes and identifying hub genes in bladder cancer based on bioinformatic analysis. BMC Urol. 21, 1-10.

Zaravinos A., Lambrou G.I., Boulalas I., Delakas D. and Spandidos D.A. (2011). Identification of common differentially expressed genes in urinary bladder cancer. PLoS One 6, e18135.

Zare M., Jazii F.R., Soheili Z.S. and Moghanibashi M.M. (2012). Downregulation of tropomyosin-1 in squamous cell carcinoma of esophagus, the role of Ras signaling and methylation. Mol. Carcinog. 51, 796-806.

Zhang J., Wang K., Zhang J., Liu S.S., Dai L. and Zhang J.-Y. (2011). Using proteomic approach to identify tumor-associated proteins as biomarkers in human esophageal squamous cell carcinoma. J. Proteome Res. 10, 2863-2872.

Zhang J., Zhang J., Xu S., Zhang X., Wang P., Wu H., Xia B., Zhang G., Lei B. and Wan L. (2018). Hypoxia-induced TPM2 methylation is associated with chemoresistance and poor prognosis in breast cancer. Cell Physiol. Biochem. 45, 692-705.

Zhao B., Baloch Z., Ma Y., Wan Z., Huo Y., Li F. and Zhao Y. (2019). Identification of potential key genes and pathways in early-onset colorectal cancer through bioinformatics analysis. Cancer Control 26, 1073274819831260.

Zhao X.-T., Zhu Y., Zhou J.-F., Gao Y.-J. and Liu F.-Z. (2021). Development of a novel 7 immune-related genes prognostic model for oral cancer: a study based on TCGA database. Oral Oncol. 112, 105088.

Zhou Y., Bian S., Zhou X., Cui Y., Wang W., Wen L., Guo L., Fu W. and Tang F. (2020). Single-cell multiomics sequencing reveals prevalent genomic alterations in tumor stromal cells of human colorectal cancer. Cancer Cell 38, 818-828. e815.

Zou Y., Wu H., Guo X., Peng L., Ding Y., Tang J. and Guo F. (2021). MK-FSVM-SVDD: a multiple kernel-based fuzzy SVM model for predicting DNA-binding proteins via support vector data description. Curr. Bioinform. 16, 274-283.

Accepted June 14, 2022